Fluctuations in Λ Multiplicity Distribution in Au+Au collisions at $\sqrt{s_{NN}} = 3.0$ GeV at STAR

Jonathan Ball [1] [2]

[1]For the STAR Collaboration

[2]University of Houston

APS April Meeting, 2021

Supported in part by

Motivation

- Continue with the study of energy dependence of Net-Λ fluctuations. (Phys. Rev. C 102, 024903 (2020))
- Continue with the comparison with Net-Proton fluctuations.

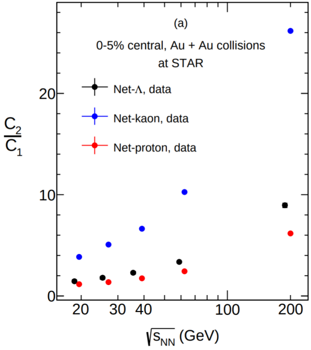

Figure 1: C_2 / C_1 energy dependence.

Cumulants of the distribution can be related with theoretical thermodynamic susceptibilities as:

$$\frac{C_2}{C_1} = \frac{\chi^B_{2,\mu}}{\chi^B_{1,\mu}}, \qquad \frac{C_3}{C_2} = \frac{\chi^B_{3,\mu}}{\chi^B_{2,\mu}}, \qquad \frac{C_4}{C_2} = \frac{\chi^B_{4,\mu}}{\chi^B_{2,\mu}}$$

Chemical freeze-out:

- Relate fluctuations with freeze-out parameters.
- Study freeze-out parameters in the context of quark-mass dependence.

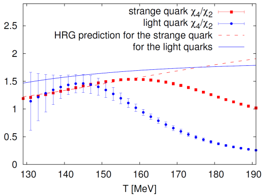

Figure 2: R. Bellwied, et. al. Phys. Rev. Lett, vol. 111, no. 20, p. 202302, 2013.

A proxy with both S and B quantum numbers, gives the opportunity to investigate not only **strangeness fluctuations** but also freeze-out parameters in the context of **quark-mass dependence**.

Net-Λ Multiplicity Distribution Fluctuations

Net-Λ multiplicity distribution measurements:

- Together with net-kaon provide a complete measurement for net-strangeness in the system after collisions.
- Λ carries both baryon and strangeness quantum numbers.

From previous work on net-Λ fluctuation analysis for the BES-I [1], the cumulant ratios C_2/C_1 and C_3/C_2 were shown as a function of $\sqrt{s_{NN}}$ and Δy

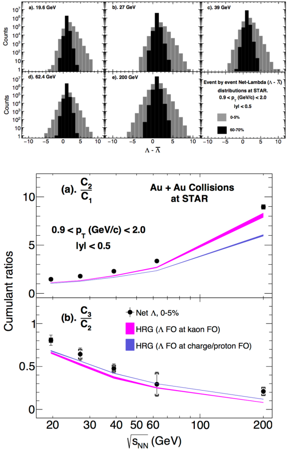

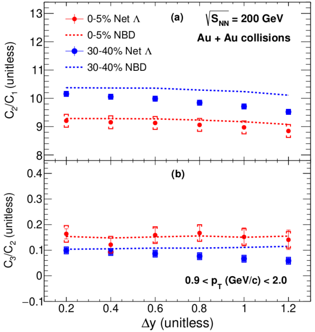

Figure 3: Δy dependence of cumulant ratios.

[1] J. Adam et al. (STAR Collaboration), Phys. Rev. C 102, 024903 (2020)

STAR FXT Setup and Analysis Information

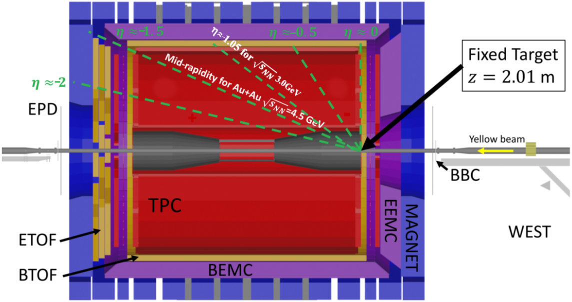

Figure 4: The convention for the analysis is beam going direction is negative direction.

Analysis Information

- **Data Set**: Run 18 FXT Au+Au $\sqrt{s_{NN}} = 3.0$ GeV
- **Events**: 308M minbias readable, 270M after cuts.

Mid-rapidity in the back-ward convention is at $y = -1.045$, the Au target is at $z = 2.01$ m.

Event Selection in Vertex Positions

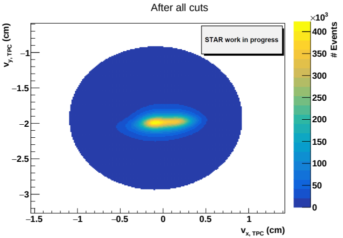

Figure 5: Vx-Vy after cuts

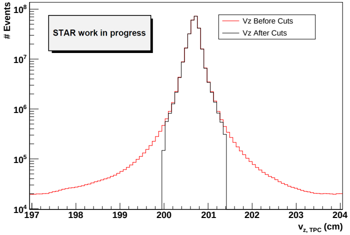

Figure 7: Vz distribution, peaked at 200.7cm. Cut ± 0.7cm

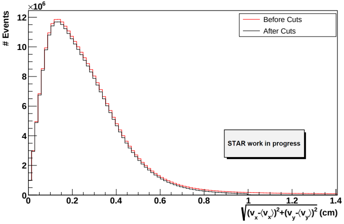

Figure 6: V_T before and after cuts

The beam is steered away from (0,0) cm. The cuts applied are for $V_T - \langle V_T \rangle$(instead of just V_T) of 1.0 cm.

Λ Particle Reconstruction

Λ reconstruction was done using the KF particle package.

The KF-Package:

- Uses the state vector $\vec{r} = (x, y, z, p_x, p_y, p_z, E, s)$ and the covariance matrix of the particles to calculate the decay vertex, momentum and energy of the mother particle.
- Instead of using DCA and pointing angle θ, it uses the χ^2-criterion, used to estimate the quality of the reconstruction.

Cuts used in KF-Package:

- DCA(PV to Λ-vertex) $<$ 1.0 cm
- DCA(p to π)$<$ 1.0 cm

Other cuts were optimized by KF-Package:

- True primary tracks are wrongly assigned as a secondary one with only 0.05% probability.
- Probability of selecting corrected fitted candidates $>$ 99.9%
- Probability that the p and π come from the same point $>$ 99.6%

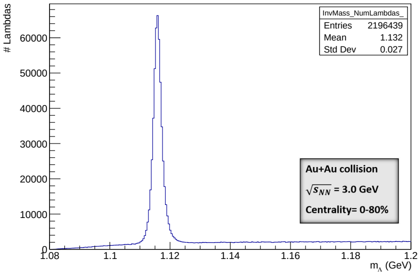

Figure 8: Λ invariant mass. $0.5 < p_T < 3.0$ GeV, $|y| < 0.5$ minimum bias.

High purity in the signal, Purity=0.98 and S/B=49

Centrality Definition

Glauber model was used to determine the centrality definition.

% Central	N_{ch} Cut
0-10	(118, 195]
10-20	(83, 118]
20-30	(58, 83]
30-40	(38, 58]
40-50	(24, 38]
50-60	(15, 24]
60-70	(8, 15]
70-80	(4, 8]

Multiplicities above 195 are excluded to avoid pile up.

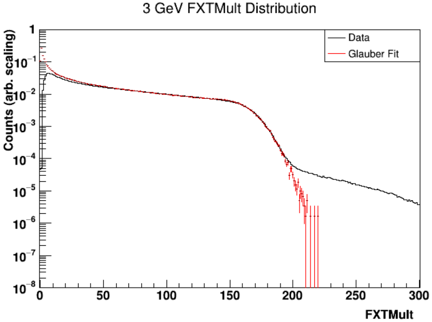

Figure 9: Primary charged particle multiplicity

FXTMult: All TPC primary charged particle multiplicity for the fixed target experiment ($\eta = [0, -2]$).

Λ Particle Acceptance

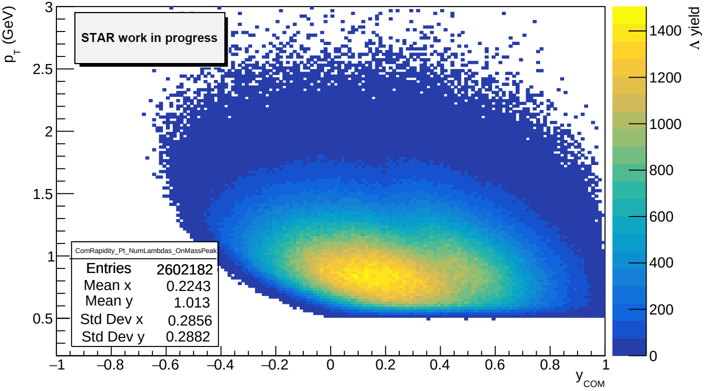

Figure 10: Lambda Acceptance

Raw Multiplicity Distribution

At $\sqrt{s_{NN}} = 3$ GeV Λ particles have low multiplicity. Fig.(11) is measured for the acceptance $(0.5 < p_T < 1.5)$ GeV and $-0.2 < y_{cm} < 1.2$.

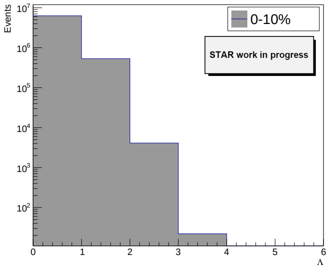

Figure 11: Λ Multiplicity Distributions for most central (0-10%)

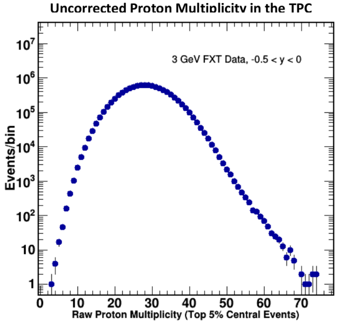

Figure 12: Raw Proton Multiplicity at $\sqrt{s_{NN}} = 3.0$ GeV.

C_2 and C_1 as a function of Δy (Uncorrected for efficiency)

Increasing the rapidity window every $\Delta y = 0.2$ for the most central collisions $(0 - 10\%)$.

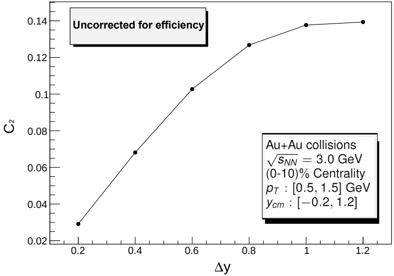

Figure 13: C_2 as a function of Δy.

- Cumulants are not efficiency corrected yet.
- Due to low Λ multiplicity a centrality dependence in the cumulants cannot be studied.
- Λ higher order cumulants (C_3, C_4, etc), at this energy might not be reliable for comparison or discussion due to low multiplicity.
- A rapidity window dependence in the cumulants can still be studied for most central collisions.
- C_1 and C_2 increase as a function of Δy consistent with central limit theorem.
- This behaviour can be used to study cumulant ratios in the context of the Λ rapidity distribution at low energies.

STAR

Qualitative Analysis: Rapidity Coverage

- Notice the strong energy dependence of dN/dy.
- Small rapidity range at low energies.

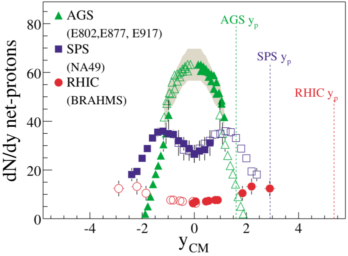

Figure 14: AGS (Au+Au at $\sqrt{s_{NN}} = 5.0$GeV), SPS (Pb+Pb at $\sqrt{s_{NN}} = 17.0$GeV), RHIC (Au+Au at $\sqrt{s_{NN}} = 200$ GeV). PhysRevLett.93.102301

- For $\sqrt{s_{NN}} = 3.0$ GeV the rapidity range is about 2.1
- Compared with $\Delta y_{max} = 1.2$ in this analysis, $\Delta y_{max} / \Delta y_{beam} \approx 0.57$

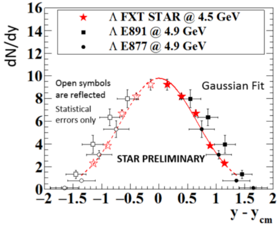

Figure 15: Λ rapidity density for FXT STAR at 4.5 GeV. Nuclear Physics A, 967(2017)808-811

Lambda rapidity range at $\sqrt{s_{NN}} = 3.0$ GeV decreased, Λ cumulant ratios should show a baryon number conservation effect when analyzed as a function of rapidity window.

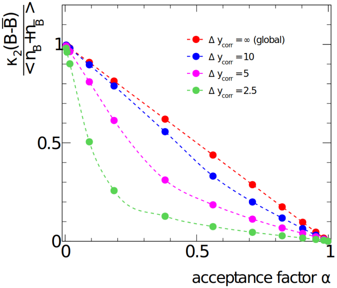

Figure 16: Normalized k_2 value as a function of accepted fraction of baryon. arXiv:1907.03032

- α is defined as the ratio between baryons inside the acceptance and baryons in full phase space $\alpha = \langle N_B \rangle / \langle N_B^{4\pi} \rangle$.
- Red line shows effect of global baryon number conservation.
- Focus only on the global baryon number conservation behaviour.

- A fast decrease in the Λ C_2/C_1 might indicate the effect in the reduction of the **rapidity range** as a function of $\sqrt{s_{NN}}$.
- This behaviour shows the effect of **global baryon conservation** for increasing Δy.
- Comparison between C_2/C_1 for $\sqrt{s_{NN}} = 200$ GeV and $\sqrt{s_{NN}} = 3$ GeV would clarify the effect of the decrease in rapidity range and baryon number conservation.

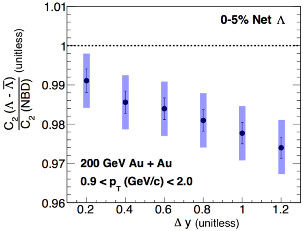

Figure 17: Rapidity-dependence of C_2 with respect to the NBD expectation. (Phys. Rev. C 102, 024903 (2020))

Summary and Future Plans

- Λ reconstruction at $\sqrt{s_{NN}} = 3.0$ GeV provides a clear signal with high purity.
- Despite the high purity in the Λ reconstruction, the multiplicity is low compared with higher energies.
- High order cumulants as a function of centrality are difficult to obtain due to low multiplicity.
- Values of cumulants up to C_2 was measured up to $\Delta y = 1.2$.

In order to continue with a quantitative analysis of the behaviour of the cumulant ratios as a function of Δy, we plan to:

- Include efficiency corrections to the calculation of C_i.
- Using particle generator models to calculate $N_B^{4\pi}$.
- Calculate $\alpha = \langle N_\Lambda \rangle \,/\, \langle N_B^{4\pi} \rangle$.

In the long term, we plan to use data from $\sqrt{s_{NN}} = 3 - 27$ GeV to map out the rapidity and centrality dependence of Λ cumulant ratios in BES-II.